

BULETINUL INSTITUTULUI POLITEHNIC DIN IAȘI
Publicat de
Universitatea Tehnică „Gheorghe Asachi” din Iași,
Tomul LX (LXIV), Fasc. 4, 2014
Secția
CONSTRUCȚII DE MAȘINI

SIZING METHODS OF AN ENGINE AIR INTAKE HOOD SCOOP

BY

VASILE-LUCIAN LEONTE¹, LIDIA GAIGINSCHI^{2*}
and IULIAN AGAPE²

¹“Alexandru Ioan Cuza” University Printing House, Iași
²“Gheorghe Asachi” Technical University of Iași,
Faculty of Mechanical Engineering

Received: December 15, 2014

Accepted for publication: December 22, 2014

Abstract. The intake process depends on the shape of geometric intake system components, operating regime of the engine but also of constructive parameters of the distribution system. In addition, for a better filling of the cylinder is necessary to optimize the parameters of the density ρ and p - external pressure supply system.

In practice, it was found that the increase at operating regime of the engine pressure difference between the outside inlet and port system the valve decreases so that the filling is flawed. Such were required the use of technical solutions capable of ensuring the pressure difference that ensures high speed filling. These technical solutions using air dynamics in motion along the bodywork and the phenomenon of inertial supercharging of intake manifold, known as **RAM** effect (Weiland, 1971; Okubo, 1986). These solutions are materialized through an intake system to which the front air inlet has a specific shape and size of the transverse surface that ensures dissemination of certain fluid flows with moving with a given speed of the car.

Key words: inlet; intake manifold; supercharging; aerodynamic flow study.

*Corresponding author; *e-mail*: lidiagaiginschi@yahoo.com

1. Introduction

In order to materialize the most convenient technical solutions it were required detailed aerodynamic body studies which were able to determine the areas characterized by high air pressure or areas where the air flow velocity is high enough to be able to ensure entry into the intake air mass flow rates capable of dynamic pressure increase.

The practice has allowed the drawing of curved isobars along some areas of the body with the help of which the planners have managed to fix location of inlet air intakes.

The figure below (Fig. 1) shows the areas specified for the isobars in the front part of a car (Aerodynamique, 1981).

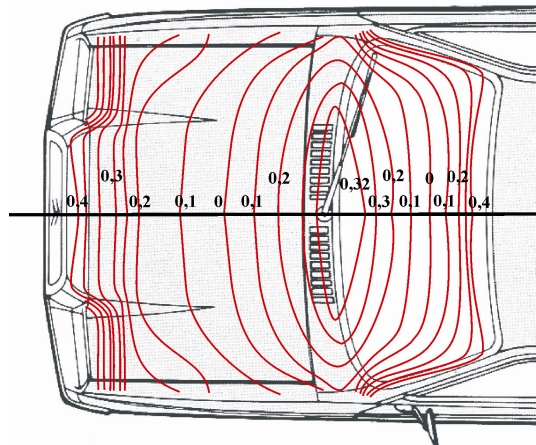


Fig. 1 – Isobars on curve surface shape front part of a car.

It can be seen that the areas located in the front of the car, at the level of the bottom of the grille, bonnet with adjustment of the front windscreen at a certain distance from the radiator grille on the bonnet and the front headlights on the lower part of the air pressure which flowed along the body exceeds the value of the atmospheric pressure. For these reasons, air intakes of the engines were located in these areas, as in the following examples (Fig. 2).

The orientation of the air intakes must be perpendicular regarding to the advancing direction of the vehicle, to be at the surface or at a certain height to it, to avoid the effect of boundary layer of fluid.

To be able to justify every solution you need constructive analysis of chart variation of the pressure of the air flow speed along the body.

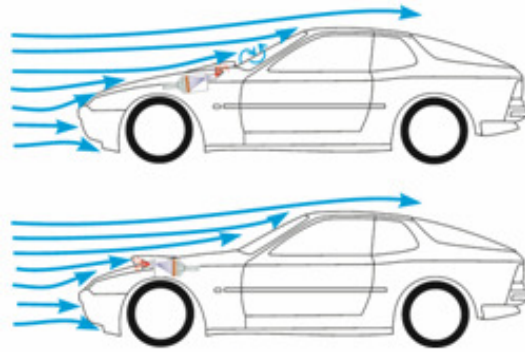


Fig. 2 – Location of inlet intakes on the surface of the body.

The figure below (Fig. 3) shows the variation of the wind pressure coefficient C_p for a randomly chosen car (<http://rennlist.com/forums/>).

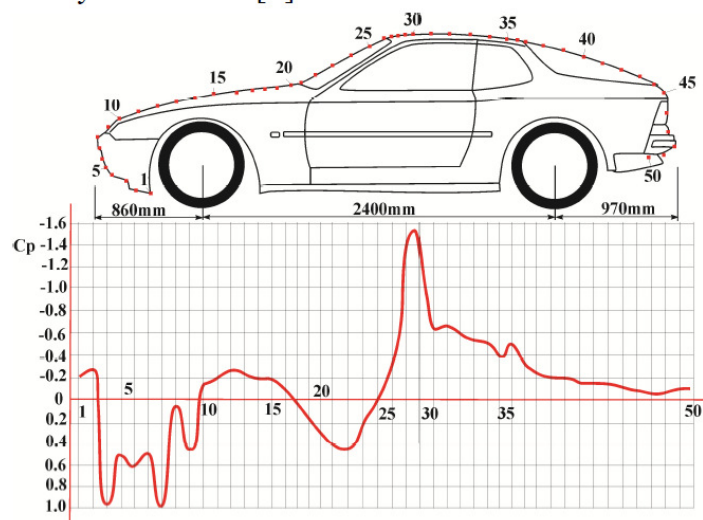


Fig. 3 – Aerodynamic coefficient of pressure variation C_p for a car.

The values of the coefficient C_p are determined in the wind tunnel, in numbered points along the bodywork; the pressures and speeds of the air in those points can be calculated. This information is necessary for determining the flow regime, with the help of Reynolds number and the thickness of the fluid layer.

Thus, in order to benefit from the increase in pressure due to air flow along the bodywork it had to be chosen items which have a value C_p with positive values. These points are 3, 5, 6, 7, 9, 16, 17, 18, 19, 20, 21, 22.

Determining the Reynolds number Re_x , it could be appreciated the flow character in that region for a certain speed so it can be determined the boundary layer

thickness at the selected point. With this information we have chosen the location and height of the area to which you must practice opening inlet of the intake air.

For example, assuming that air flow influence makes itself felt from the speed of 60 km/h up to the maximum speed of the vehicle, the Re_x is calculated for areas of the body above. Table 1 analysis the results.

Table 1

Physical Parameters of the Air Flow Along a Bodywork, the Aerodynamic Flow Study

Poz	x [m]	v_∞ [m/s]	C_p	v [m/s]	p KPA	[%] p	Re_x	The character of flow	δ [m]
3	0.26	16.6	0.6	10.49	100.101	0.1	$2.858 \cdot 10^5$	laminar	0.0024
		19.4	0.6	12.27	100.138	0.13	$3.34^5 \cdot 10$	laminar	0.0022
		22.2	0.6	14.04	100.181	0.18	$3.82 \cdot 10^5$	laminar	0.00206
		25	0.6	15.8	100.23	0.23	$4.30 \cdot 10^5$	laminar	0.00195
		27.7	0.6	17.52	100.28	0.28	$4.76 \cdot 10^5$	laminar	0.00185
		30.5	0.6	19.29	100.34	0.34	$5.25 \cdot 10^5$	turbulent	0.00712
		33.3	0.6	21.06	100.407	0.407	$5.73 \cdot 10^5$	turbulent	0.007
		36.1	0.6	22.83	100.478	0.478	$6.21 \cdot 10^5$	turbulent	0.0069
		38.8	0.6	24.54	100.553	0.553	$6.68 \cdot 10^5$	turbulent	0.0068
		41.6	0.6	26.3	100.635	0.635	$7.17 \cdot 10^5$	turbulent	0.0067
5	0.09	16.6	1	0	100.168	0.17	$0.99 \cdot 10^5$	laminar	0.0014
		19.4	1	0	100.230	0.23	$1.15 \cdot 10^5$	laminar	0.0013
		22.2	1	0	100.302	0.3	$1.32 \cdot 10^5$	laminar	0.0012
		25	1	0	100.383	0.38	$1.49 \cdot 10^5$	laminar	0.0011
		27.7	1	0	100.470	0.47	$1.65 \cdot 10^5$	laminar	0.00108
		30.5	1	0	100.570	0.57	$10^5 \cdot 1.82$	laminar	0.00103
		33.3	1	0	100.680	0.68	$1.98 \cdot 10^5$	laminar	0.00099
		36.1	1	0	100.798	0.79	$2.15 \cdot 10^5$	laminar	0.00095
		38.8	1	0	100.922	0.92	$2.31 \cdot 10^5$	laminar	0.00092
		41.6	1	0	101.060	1.06	$2.48 \cdot 10^5$	laminar	0.00088
6	0.06	16.6	0.92	4.69	100.155	0.15	$0.65 \cdot 10^5$	laminar	0.0011
		19.4	0.92	5.48	100.212	0.21	$0.77 \cdot 10^5$	laminar	0.00106
		22.2	0.92	6.28	100.277	0.27	$0.88 \cdot 10^5$	laminar	0.00099
		25	0.92	7.07	100.352	0.35	$0.99 \cdot 10^5$	laminar	0.00093
		27.7	0.92	7.83	100.432	0.432	$1.10 \cdot 10^5$	laminar	0.00088
		30.5	0.92	8.62	100.524	0.52	$1.21 \cdot 10^5$	laminar	0.00084
		33.3	0.92	9.41	100.625	0.62	$1.32 \cdot 10^5$	laminar	0.00081
		36.1	0.92	10.21	100.734	0.734	$1.43 \cdot 10^5$	laminar	0.00078
		38.8	0.92	10.97	100.848	0.84	$1.54 \cdot 10^5$	laminar	0.00075
		41.6	0.92	11.76	100.975	0.97	$1.65 \cdot 10^5$	laminar	0.00072

Table 1
Continuation

Poz	x [m]	v_{∞} [m/s]	C_p	v [m/s]	p KPA	[%] p	Re_x	The character of flow	δ [m]
7	0.04	16.6	0.8	7.42	100.135	0.13	$0.44 \cdot 10^5$	laminar	0.0009
		19.4	0.8	8.67	100.184	0.18	$0.51 \cdot 10^5$	laminar	0.00087
		22.2	0.8	9.93	100.241	0.24	$0.58 \cdot 10^5$	laminar	0.00081
		25	0.8	11.18	100.306	0.30	$0.66 \cdot 10^5$	laminar	0.00076
		27.7	0.8	12.38	100.375	0.38	$0.73 \cdot 10^5$	laminar	0.00072
		30.5	0.8	13.64	100.456	0.46	$0.80 \cdot 10^5$	laminar	0.00069
		33.3	0.8	14.89	100.543	0.54	$0.88 \cdot 10^5$	laminar	0.0066
		36.1	0.8	16.14	100.638	0.64	$0.96 \cdot 10^5$	laminar	0.00063
		38.8	0.8	17.35	100.737	0.74	$1.03 \cdot 10^5$	laminar	0.00061
41.6	0.8	18.6	100.848	0.85	$1.10 \cdot 10^5$	laminar	0.00059		
9	0.12	16.6	0.4	12.8	100.067	0.07	$1.32 \cdot 10^5$	laminar	0.0016
		19.4	0.4	15.02	100.092	0.09	$1.54 \cdot 10^5$	laminar	0.0015
		22.2	0.4	17.19	100.120	0.12	$1.76 \cdot 10^5$	laminar	0.0014
		25	0.4	19.36	100.153	0.15	$1.98 \cdot 10^5$	laminar	0.0013
		27.7	0.4	21.45	100.188	0.18	$2.20 \cdot 10^5$	laminar	0.00125
		30.5	0.4	23.62	100.228	0.22	$2.42 \cdot 10^5$	laminar	0.00119
		33.3	0.4	25.79	100.271	0.27	$2.64 \cdot 10^5$	laminar	0.00114
		36.1	0.4	27.96	100.319	0.32	$2.86 \cdot 10^5$	laminar	0.00110
		38.8	0.4	30.05	100.369	0.37	$3.08 \cdot 10^5$	laminar	0.00106
41.6	0.4	32.22	100.424	0.42	$3.30 \cdot 10^5$	laminar	0.00102		
16	1.15	16.6	-0.1	17.4	99.983	-0.02	$1.29 \cdot 10^6$	turbulent	0.026
		19.4	-0.1	20.3	99.977	-0.023	$1.50 \cdot 10^6$	turbulent	0.0255
		22.2	-0.1	23.3	99.969	-0.031	$1.72 \cdot 10^6$	turbulent	0.0248
		25	-0.1	26.2	99.962	-0.039	$1.94 \cdot 10^6$	turbulent	0.0242
		27.7	-0.1	29.0	99.953	-0.047	$2.15 \cdot 10^6$	turbulent	0.0238
		30.5	-0.1	31.9	99.943	-0.057	$2.37 \cdot 10^6$	turbulent	0.0233
		33.3	-0.1	34.9	99.932	-0.068	$2.58 \cdot 10^6$	turbulent	0.0229
		36.1	-0.1	37.8	99.920	-0.08	$2.80 \cdot 10^6$	turbulent	0.0225
		38.8	-0.1	40.7	99.907	-0.093	$3.01 \cdot 10^6$	turbulent	0.0222
41.6	-0.1	43.6	99.894	-0.11	$3.23 \cdot 10^6$	turbulent	0.0219		
17	1.27	16.6	0	16.6	100.000	0	$1.39 \cdot 10^6$	turbulent	0.0286
		19.4	0	19.4	100.000	0	$1.63 \cdot 10^6$	turbulent	0.0277
		22.2	0	22.2	100.000	0	$1.86 \cdot 10^6$	turbulent	0.0270
		25	0	25	100.000	0	$2.10 \cdot 10^6$	turbulent	0.0264
		27.7	0	27.7	100.000	0	$2.33 \cdot 10^6$	turbulent	0.0258
		30.5	0	30.5	100.000	0	$2.56 \cdot 10^6$	turbulent	0.0253
		33.3	0	33.3	100.000	0	$2.80 \cdot 10^6$	turbulent	0.0249
		36.1	0	36.1	100.000	0	$3.03 \cdot 10^6$	turbulent	0.0245
		38.8	0	38.8	100.000	0	$3.26 \cdot 10^6$	turbulent	0.0241
41.6	0	41.6	100.000	0	$3.49 \cdot 10^6$	turbulent	0.0238		

Table 1
Continuation

Poz	x [m]	v_{∞} [m/s]	C_p	v [m/s]	p KPA	[%] p	Re_x	The character of flow	δ [m]
18	1.37	16.6	0.1	15.75	100.017	0.017	$1.50 \cdot 10^6$	turbulent	0.0014
		19.4	0.1	18.40	100.023	0.023	$1.76 \cdot 10^6$	turbulent	0.0013
		22.2	0.1	21.06	100.030	0.03	$2.01 \cdot 10^6$	turbulent	0.0012
		25	0.1	23.71	100.038	0.038	$2.26 \cdot 10^6$	turbulent	0.0011
		27.7	0.1	26.28	100.047	0.047	$2.51 \cdot 10^6$	turbulent	0.00108
		30.5	0.1	28.93	100.057	0.057	$2.76 \cdot 10^6$	turbulent	0.00103
		33.3	0.1	31.59	100.068	0.068	$3.02 \cdot 10^6$	turbulent	0.00099
		36.1	0.1	34.25	100.079	0.079	$3.27 \cdot 10^6$	turbulent	0.00095
		38.8	0.1	36.81	100.092	0.092	$3.52 \cdot 10^6$	turbulent	0.00092
41.6	0.1	39.46	100.106	0.106	$3.77 \cdot 10^6$	turbulent	0.00088		
19	1.47	16.6	0.2	14.84	100.033	0.033	$1.61 \cdot 10^6$	turbulent	0.0322
		19.4	0.2	17.35	100.046	0.046	$1.88 \cdot 10^6$	turbulent	0.0312
		22.2	0.2	19.85	100.060	0.060	$2.16 \cdot 10^6$	turbulent	0.0303
		25	0.2	22.36	100.076	0.076	$2.43 \cdot 10^6$	turbulent	0.0296
		27.7	0.2	24.77	100.094	0.094	$2.69 \cdot 10^6$	turbulent	0.0290
		30.5	0.2	27.28	100.114	0.114	$2.96 \cdot 10^6$	turbulent	0.0285
		33.3	0.2	29.78	100.136	0.136	$3.24 \cdot 10^6$	turbulent	0.0280
		36.1	0.2	32.28	100.160	0.160	$3.51 \cdot 10^6$	turbulent	0.0275
		38.8	0.2	34.70	100.184	0.184	$3.77 \cdot 10^6$	turbulent	0.0271
41.6	0.2	37.21	100.212	0.212	$4.05 \cdot 10^6$	turbulent	0.0268		
20	1.57	16.6	0.3	13.88	100.050	0.05	$1.72 \cdot 10^6$	turbulent	0.034
		19.4	0.3	16.23	100.069	0.07	$2.01 \cdot 10^6$	turbulent	0.033
		22.2	0.3	18.57	100.090	0.09	$2.31 \cdot 10^6$	turbulent	0.032
		25	0.3	20.92	100.115	0.11	$2.59 \cdot 10^6$	turbulent	0.031
		27.7	0.3	23.17	100.141	0.14	$2.88 \cdot 10^6$	turbulent	0.0306
		30.5	0.3	25.51	100.171	0.17	$3.17 \cdot 10^6$	turbulent	0.0300
		33.3	0.3	27.86	100.203	0.20	$3.46 \cdot 10^6$	turbulent	0.0295
		36.1	0.3	30.20	100.239	0.24	$3.75 \cdot 10^6$	turbulent	0.0290
		38.8	0.3	32.46	100.276	0.27	$4.03 \cdot 10^6$	turbulent	0.0286
41.6	0.3	34.80	100.318	0.32	$4.32 \cdot 10^6$	turbulent	0.0282		
21	1.67	16.6	0.4	12.8	100.067	0.07	$1.83 \cdot 10^6$	turbulent	0.0356
		19.4	0.4	15.02	100.092	0.09	$2.14 \cdot 10^6$	turbulent	0.0345
		22.2	0.4	17.19	100.120	0.12	$2.45 \cdot 10^6$	turbulent	0.0336
		25	0.4	19.36	100.153	0.15	$2.76 \cdot 10^6$	turbulent	0.0328
		27.7	0.4	21.45	100.188	0.18	$3.06 \cdot 10^6$	turbulent	0.0321
		30.5	0.4	23.62	100.228	0.22	$3.37 \cdot 10^6$	turbulent	0.0315
		33.3	0.4	25.79	100.271	0.27	$3.68 \cdot 10^6$	turbulent	0.0310
		36.1	0.4	27.96	100.319	0.32	$3.99 \cdot 10^6$	turbulent	0.0305
		38.8	0.4	30.05	100.369	0.37	$4.29 \cdot 10^6$	turbulent	0.030
41.6	0.4	32.22	100.424	0.42	$4.60 \cdot 10^6$	turbulent	0.0296		

Table 1
Continuation

Poz	x [m]	v_{∞} [m/s]	C_p	v [m/s]	p KPA	[%] p	Re_x	The character of flow	δ [m]
22	1.77	16.6	0.45	12.31	100.076	0.07	$1.94 \cdot 10^6$	turbulent	0.037
		19.4	0.45	14.38	100.103	0.103	$227 \cdot 10^6$	turbulent	0.036
		22.2	0.45	16.46	100.136	0.13	$260 \cdot 10^6$	turbulent	0.035
		25	0.45	18.54	100.172	0.17	$2.93 \cdot 10^6$	turbulent	0.034
		27.7	0.45	20.54	100.211	0.21	$3.24 \cdot 10^6$	turbulent	0.0337
		30.5	0.45	22.62	100.256	0.25	$3.57 \cdot 10^6$	turbulent	0.0330
		33.3	0.45	24.69	100.306	0.30	$3.90 \cdot 10^6$	turbulent	0.0325
		36.1	0.45	26.77	100.359	0.36	$4.23 \cdot 10^6$	turbulent	0.0319
		38.8	0.45	28.77	100.415	0.41	$4.54 \cdot 10^6$	turbulent	0.0315
		41.6	0.45	30.85	100.477	0.47	$4.87 \cdot 10^6$	turbulent	0.031

From the analysis of the data processed in the table we can determine the most favorable area location for air intake plugs. Thus, items 5, 6, 7 and 19 are characterized by increases in values of local pressures from atmospheric pressure at high speeds, with the percentage up to 1%, using sockets in these areas of apparent air intake, arranged perpendicular to the direction of movement and located at a height, towards the area of flow, equal to or greater than the limit thickness of fluid.

In areas corresponding to the points 16 and 17, where air pressure is zero growth, the placed air intakes operate on the principle of growth associated with increasing the speed of air flow over those areas.

Because the effect of dynamic air supercharging corresponds in substance to the frontal surface, the sizing of the intake air is required so that the fluid flow by intake system, at the range of speeds with which the car can run, to be superior, with certain percentages, to the fresh fluid flow by thermal processes that take place in the engine.

In designing the shape of the air inlet, outlets have taken in account, in addition to the requirements related to aerodynamics, linear load losses entered.

Thus, there were experimentally determined characteristic forms of inlet intakes whose entries lead to low losses. It started from the entrance of an unrounded pipe and optimizations have been made to reduce the losses of load.

2. Sizing Methods of an Engine Air Intake Hood Scoop

The sizing of the front surface of the intake is based on calculating air flow to be perpetuated by the engine inlet system. For this it is necessary to determine fresh air intake of the engine, depending on the speed of movement. Thus, the air flow that is going through intakes must be higher than the air flow consumed by the engine, in order to recover debt and losses that take place

along the route of intake. To be able to benefit from the effect of RAM inertional filling we must choose a flow approximately 35-50% higher than the total theoretical flow rate which the engine would consume in ideal conditions, in order to get a certain power to enable it to run with maximum speed.

Thus, with the help of constructive and functional parameters we could express the flow rate of fresh air consumed by the engine \mathbf{m}_L , as follows:

$$\mathbf{m}_L = \frac{6.33 V_t \eta_v n \rho_a \lambda m_{L0}}{(1 + \lambda m_{L0}) \Delta \alpha_a}, \text{ [kg/h]} \quad (1)$$

$$\mathbf{m}_L = \frac{0.001758 V_t \eta_v n \rho_a \lambda m_{L0}}{(1 + \lambda m_{L0}) \Delta \alpha_a}, \text{ [kg/s]} \quad (2)$$

where: V_t – total engine capacity, expressed in (l); η_v – the return filling; n – engine speed (RPM); ρ_a – fresh air density (1.225 kg/m³); λ – excess air coefficient; m_{L0} – the minimum amount of air necessary for combustion of one kilogram (kg) fuel; $\Delta \alpha_a$ – angular duration of the intake process (degree-crankshaft rotations).

The formula for the calculation of the mass flow rate of the air consumed by the engine shows its dependence on operation speed.

At certain revs, through the gearbox are obtained certain travel speeds depending on the gear ratios and tire rolling radius.

For example, to run at a speed v_1 , the engine of a motor vehicle works at speed n_1 , consuming \mathbf{m}_{L1} fresh air. Knowing the gearbox transmission ratio and the rolling radius of the tire it can be written:

$$v_1 = \frac{n_1}{r_{trf} r_{trI,II,III,IV,V}} \frac{\pi}{30} r_{rulare}, \text{ [m,s]} \quad (3)$$

where: r_{trf} – is the gear ratio of the differential; $r_{trI,II,III,IV}$ – is the gear transmission ratio of the step at which it is obtained the desired speed; r_{rulare} – is the radius of the tire (m).

With these data you can select the cross-section of the intake, so the circulated air mass flow rate exceeds the flow requirements by the engine.

We can thus express mathematically the condition previously imposed in the form of:

$$\rho_a v_1 S_1 = \mathbf{m}_L \quad (4)$$

and it can be obtained the expression of the necessary air intake section as follows:

$$S_{\text{final}} = \frac{(1.35 \div 1.50)m_L}{\rho_a v_1}, \text{ [m}^2\text{]} \quad (5)$$

To be able to evidenciate the increase of mass flow supplied by air intakes, a table shall be drawn up, which analyzes the flow rate of fresh fluid consumed by the engine and socket provided intake flow rate for different car speeds.

As a result of data processing, it is found that the necessary minimum cross section is determined for a speed value far below the maximum speed. In our example, it is found that for a travel speed of 80 km/h in 4th gear gearbox, to obtain the air flow consumed by the engine it is necessary an area of the air intake opening whose value exceeds the similar surface required if running at full speed.

The condition should be adopted by the

$$S_{\text{final}} = (1.35 \div 1.50) \cdot S_1, \text{ [m}^2\text{]} \quad (6)$$

With this adopted rule, the intake air section for the studied automobile is $S = 0.00256 \text{ m}^2$. Thus it ensures the optimal condition for the inertional filling at low speeds by obtaining a debit spread through air intake higher than the consumed one. At high speeds, the flow through the intake air is much greater than that required. This growing mass flow covers the losses that occur along the inlet system in case of operation with high revs. For a better view of the effects of choosing a corresponding value for the cross section of the intake air, is plotted the variation of mass flow consumed by the engine, the required minimum cross section of the intake, and air mass flow circulated through the air intake, depending on speed of the vehicle.

From these theoretical findings it can be chosen various constructive forms of the air intakes, from the circular shape, continuing with various rectangular shapes. In order to ensure a proper efficiency of the system, must take into account the minimum dynamic pressure losses that may enter the inlet cross-sectional shape of the intake air.

In conjunction with the aerodynamic studies which determined the boundary layer thickness, fluid flow, air velocity and pressure distribution over the body, there can be identified constructive solutions which do not increase the aerodynamic drag resistance.

If we choose for the beginning a circular cross-section, its surface is equal to

$$S = \frac{\pi d^2}{4} \quad (7)$$

Using other geometric shapes (Fig. 4) in order to get the same cross section value, we notice the advantages of rectangular forms, regarding to drag

resistance in conjunction with simpler integration in bodywork components. In terms of aerodynamic, the circular or rectangular section of the air intakes offers low losses just through their integration on certain areas of the body, the entry of air being at the boundary layer. If these air intakes would be apparent, exceeding the height limit layer of fluid, then it would create additional aerodynamic resistance. In this situation is needed the use of rectangular shapes whose ratio between width and height should be reduced.

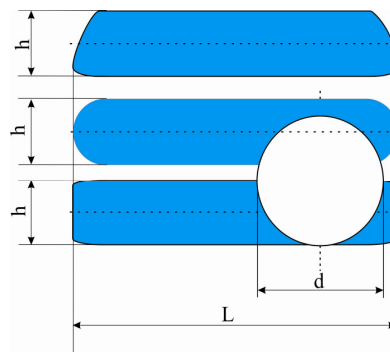


Fig. 4 – Constructive forms for intakes.

From aerodynamic point of view, the intake system that uses the principle of dynamic supercharging with fresh fluid works as a Venturi nozzle, either positive, in order to facilitate the reduction of flow velocity and pressure increase, either negative, in order to encourage increased speed of flow, favoring the effect of inertional filling and conveying greater fluid flow, or negative-positive combined, the aim being to achieve a recovery of pressure drop in minimum flow section. The following illustrations (Fig. 5) are distinct situations of Venturi type intake system and pressure-velocity parameters variation with aerodynamic coefficient C_p (Katz, 1996).

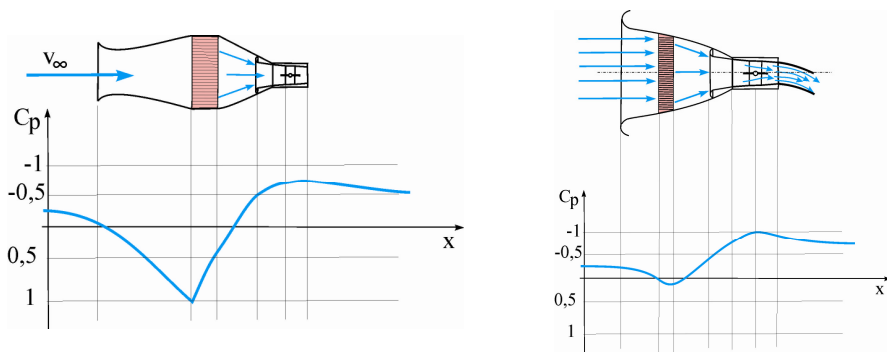


Fig. 5 – Types of inlet Venturi type systems and pressure-velocity variation function of aerodynamic pressure coefficient C_p .

3. Constructive Solutions for Intakes Hood Scoop

The solution presented takes into account the amount of air pressure in the stagnation flow on the front of the body. Located at the lower level or higher of the headlights on the front surface of the air flow on the hood, intakes do not introduce additional aerodynamic loss in addition to ensuring a higher pressure flow of air, and conveying a fresh fluid flow superior to the one required by the engine, by selecting the appropriate geometric dimensions (Simcox, 2002; Wayne, 1992; Horney & Knowles, 1999; Telly, 2009; Ivy Croft, 2007; Fiello & Williams, 2011; Smith, 2007; Silvano, 2010; Khouw *et al.*, 2006; Knapp, 1993; Teraguchi & Okagawa, 2012).

Intake system can function as a Venturi negative, due to the choice of the form of the frontal and lateral surfaces, which contribute to increasing the speed of air flow.

In Fig. 6 are presented some constructive solutions that use this type of system.

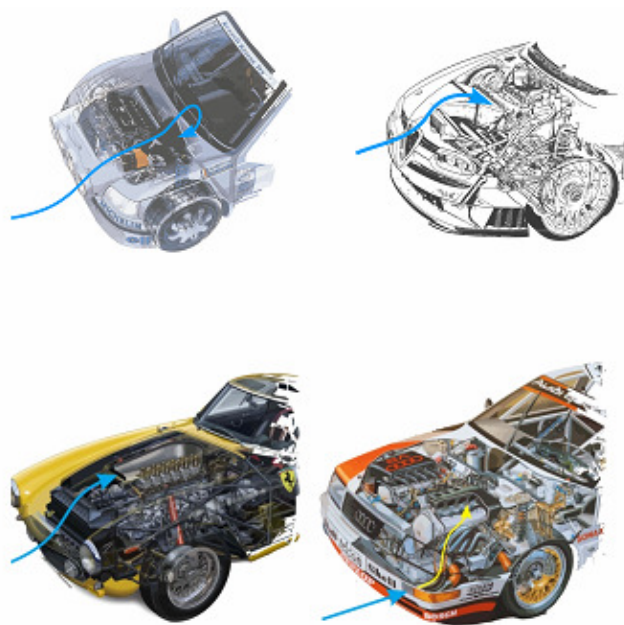


Fig. 6 – types of air intakes and their location on the body.

4. Conclusions

Aerodynamic intake inlet supercharger systems contribute to the increase in performances of dynamic internal combustion engines by flattening the curve of maximum torque. Also, these intake systems contribute to the

reduction of specific fuel consumption due to the filling of the cylinders of the engine with a denser mixture due to the air inlet from the outside of the engine compartment. The fact that designed intake systems provide inertional filling at low speeds of movement lead to raising the value of the corresponding engine timing rotation of crankshaft.

REFERENCES

- * * *Aerodynamique, Double Chevron # 59*, Relations Publiques Citroen, Edition 10.2.1981.
- Fiello J.R., Williams S., *Hood air Scoop*. United States Patent Application Publication, U.S. 8029606 B2/2011.
- Horney K., Knowles T.M., *Fresh Air Duct System for a Vehicle*. United States Patent Application Publication, U.S. 5860685 A/1999.
<http://rennlist.com/forums/924-931-944-951-968-forum/476932-aerodynamic-balance-of-a-944-a.html>
- Ivy Croft A., *Cold Air Intake*. United States Design Patent, USD 555172 S1/2007.
- Katz J., *Race Car Aerodynamics, Designing for Speed*. Bentley Publishers, 1996.
- Khouw R., Chapman R., Hagiwara T., *Automobile Over Bulkhead Air Intake System*. United States Patent Application Publication, U.S. 20060006012 A1/2006.
- Knapp F.J., *Air Cleaner and Snorkel Assembly*. United States Patent Application Publication, U.S. 5195484 A/1993.
- Okubo J., *Inertia Supercharger for Internal Combustion Engines*. United States Patent Application Publication, U.S. 4515115 A, 1986.
- Silvano P., *Intake System for a Vehicle*. United States Patent Application Publication, U.S. 8516986 B2/2010.
- Simcox G., *Automotive Hood Scoop*. United States Design Patent, USD 457471 S1/2002.
- Smith R., *External Air Scoop for Internal Combustion Engine Air Intake of an Automobile*. United States Patent Application Publication, U.S. 20080083575 A1/2007.
- Telly W., *Apparatus and Method for Boosting Engine Performance*. United States Patent Application Publication, U.S. 7597088 B2/2009.
- Teraguchi S., Okagawa Y., *Intake Air Introducing Structure for Automobile*. United States Patent Application Publication, U.S. 8127878 B2/2012.
- Wayne M., *Hood Scoop Assembly*. United States Patent Application Publication, U.S. 5157377 A, 1992.
- Weiland P., *High RAM Manifold*. United States Patent Application Publication, U.S. 3561408 A, 1971.

METODE DE PROIECTARE A PRIZELOR DE ADMISIE A AERULUI
PENTRU UN MOTOR CU ARDERE INTERNĂ

(Rezumat)

Procesul de admisie depinde de forma geometrică a componentelor sistemului de admisie, regimul de funcționare al motorului cât și de parametrii constructivi ai sistemului de distribuție. În plus, pentru o mai bună umplere a cilindrului este necesar să se optimizeze parametrii privind densitatea și presiunea furnizate din exterior.

În practică, s-a constatat că odată cu creșterea regimului de exploatare al motorului diferența de presiune dintre exteriorul sistemului de admisie și portul supapei scade, fapt pentru care umplerea devine defectuoasă. Astfel a fost necesară utilizarea unor soluții tehnice capabile să asigure o diferență de presiune care să asigure umplerea la turații ridicate. Aceste soluții tehnice utilizează dinamica aerului în mișcare de-a lungul caroseriei și fenomenul supraalimentării inerționale din galeriile de admisie, cunoscut ca efectul **RAM** (Weiland, 1971; Okubo, 1986). Aceste soluții sunt materializate printr-un sistem de admisie la care partea frontală de admisie a aerului are o anumită formă și dimensiune a suprafeței transversale care asigură vehicularea anumitor debite de fluid odată cu deplasarea cu o anumită viteză a automobilului.